

Self-trapping DCM by the host deformation in flexible host-guest molecules

Le-Ping Miao, Qi Qi, Xiang-Bin Han,* Wen Zhang*

Jiangsu Key Laboratory for Science and Applications of Molecular Ferroelectrics and School of Chemistry and Chemical Engineering, Southeast University, Nanjing 211189, China

* E-mail: hanxiangbin@seu.edu.cn

zhangwen@seu.edu.cn

Experimental

Figure S1. Room-temperature powder X-ray diffraction of **1**·CH₂Cl₂, **1**·dioxane, and **1**·DMF.

Figure S2. Two-site disorders of α -CH₂Cl₂ and β -CH₂Cl₂ molecules and one *tert*-butyl group of **1**·CH₂Cl₂.

Figure S3. Atomic contacts to the Hirshfeld surface of the [Zn₂(saloph)] of crystals **1**·CH₂Cl₂, **1**·dioxane, and **1**·DMF.

Figure S4. Intermolecular interactions between the guest and host and Hirshfeld surface analysis together with fingerprint plots of (a) **1**·CH₂Cl₂, (b) **1**·dioxane, and (c) **1**·DMF at 100 K. H atoms involved in the interactions are shown in orange. The blue, white, and red regions of the surfaces correspond to negative, neutral, and positive (close contact) isoenergy, respectively.

Figure S5 (a) The XRD pattern of the desolvated form from **1**·DMF measured with Kapton film protection (red curve) and in ambient (black curve). The re-adsorption experiment for dioxane (b) and DMF (c). The desolvate compound **1** was placed under the dioxane vapor (433 K) and DMF vapor (433 K) for 2h. After that, XRD measurement was employed to check the final component. Compound **1** can't turn back to **1**·dioxane, and it can turn back to **1**·DMF.

Figure S6 The UV-vis diffuse reflectance spectra (a) and the excitation spectra (b) of three compounds.

Figure S7 The calculated HOMO and LUMO for three compounds.

Table S1. Crystallographic data and structure refinement details for **1**·CH₂Cl₂, **1**·dioxane, and **1**·DMF.

Table S2. Selected bond lengths [Å] and angles [°] for **1**·CH₂Cl₂ (100 K, 373 K), **1**·dioxane (100 K), and **1**·DMF (100 K).

Table S3. The value of natural cavities and solvent molecules occupied volume of **1·CH₂Cl₂**, **1·dioxane**, and **1·DMF** calculated by Platon.

Experiment

Materials and general characterizations.

Reagents used were in analytical grade without further purification.

Thermogravimetric analysis (TGA) was performed by an SDT-Q600 system (NETZSCH). The crystals were filtered out from the solution, and the remaining solvent was removed with tissue without any further drying treatment. And the TG test was started within one hour to avoid the solvent loss caused by experiment errors.

Powder X-ray diffraction patterns were obtained on a Rigaku SmartLab X-ray diffraction instrument. Single-crystal X-ray Diffraction was collected on a Rigaku Oxford Diffraction Supernova Dual Source, Cu at Zero equipped with an AtlasS2 CCD using Cu K α radiation and Rigaku Oxford Diffraction XtaLAB Synergy R, DW system equipped with an HyPix using Mo K α radiation. The CrysAlisPro software package was used to collect Data, refine cells, and reduce data. The SHELXL-2014 software package was used to solve the structures by direct methods and successive Fourier synthesis and full-matrix least-squares refinements on F^2 . All non-hydrogen atoms were refined anisotropically.

Solid powder UV absorption spectrum was used as a UV-visible spectrophotometer (UV-2600, Shimadzu). Solid-state emission spectra were collected on a steady-state, transient fluorescence spectrometer (PluoroLog 3-TCSPC, Horiba Jobin Yvon Inc).

Time-dependent density functional theory (TD-DFT) calculations of **1-DCM**, **1·dioxane**, and **1-DMF** were performed within Gaussian09 Package². A single molecular unit with solvent was extracted and calculated their absorption properties using the TD -B3LYP/6-31G* method.

Synthesis. The synthesis of Zn(saloph) was reported in the procedure.¹ Red block crystals of **1·CH₂Cl₂** were obtained by a slow evaporation of a mixed DCM-CH₃CN (v:v = 10:1) solution of [Zn₂(saloph)] (0.5 g, 0.88 mmol) and quinuclidine (0.2 g, 1.77 mmol), with a yield of 72% (based on quinuclidine). Compound **1·dioxane** and **1·DMF** were prepared with a similar method with a yield of 65% through DCM-dioxane (v:v = 1:1) and DCM-DMF (v:v = 1:1), respectively.

CCDC 2052505–2052510 and 2064699–2064700 contains the crystallographic data for **1·CH₂Cl₂**,

1·dioxane, and **1·DMF**. These data can be obtained free of charge via <http://www.ccdc.cam.ac.uk/conts/retrieving.html>, or from the Cambridge Crystallographic Data Centre, 12 Union Road, Cambridge CB2 1EZ, UK; fax: +44 1223-336-033; or e-mail: deposit@ccdc.cam.ac.uk.

References

1. Kleij, A. W.; Kuil, M.; Tooke, D. M.; Lutz, M.; Spek, A. L.; Reek, J. N. H. Zn^{II}–Salphen Complexes as Versatile Building Blocks for the Construction of Supramolecular Box Assemblies. *Chem. Eur. J.* **2005**, *11*, 4743–4750.
2. Frisch, M. J.; Trucks, G. W.; Schlegel, H. B.; Scuseria, G. E.; Robb, M. A.; Cheeseman, J. R.; Scalmani, G.; Barone, V.; Petersson, G. A.; Nakatsuji, H.; Li, X.; Caricato, M.; Marenich, A. V.; Bloino, J.; Janesko, B. G.; Gomperts, R.; Mennucci, B.; Hratchian, H. P.; Ortiz, J. V.; Izmaylov, A. F.; Sonnenberg, J. L.; Williams; Ding, F.; Lipparini, F.; Egidi, F.; Goings, J.; Peng, B.; Petrone, A.; Henderson, T.; Ranasinghe, D.; Zakrzewski, V. G.; Gao, J.; Rega, N.; Zheng, G.; Liang, W.; Hada, M.; Ehara, M.; Toyota, K.; Fukuda, R.; Hasegawa, J.; Ishida, M.; Nakajima, T.; Honda, Y.; Kitao, O.; Nakai, H.; Vreven, T.; Throssell, K.; Montgomery Jr., J. A.; Peralta, J. E.; Ogliaro, F.; Bearpark, M. J.; Heyd, J. J.; Brothers, E. N.; Kudin, K. N.; Staroverov, V. N.; Keith, T. A.; Kobayashi, R.; Normand, J.; Raghavachari, K.; Rendell, A. P.; Burant, J. C.; Iyengar, S. S.; Tomasi, J.; Cossi, M.; Millam, J. M.; Klene, M.; Adamo, C.; Cammi, R.; Ochterski, J. W.; Martin, R. L.; Morokuma, K.; Farkas, O.; Foresman, J. B.; Fox, D. J. In *Gaussian 09 Rev. B.02*, Wallingford, CT, 2009.

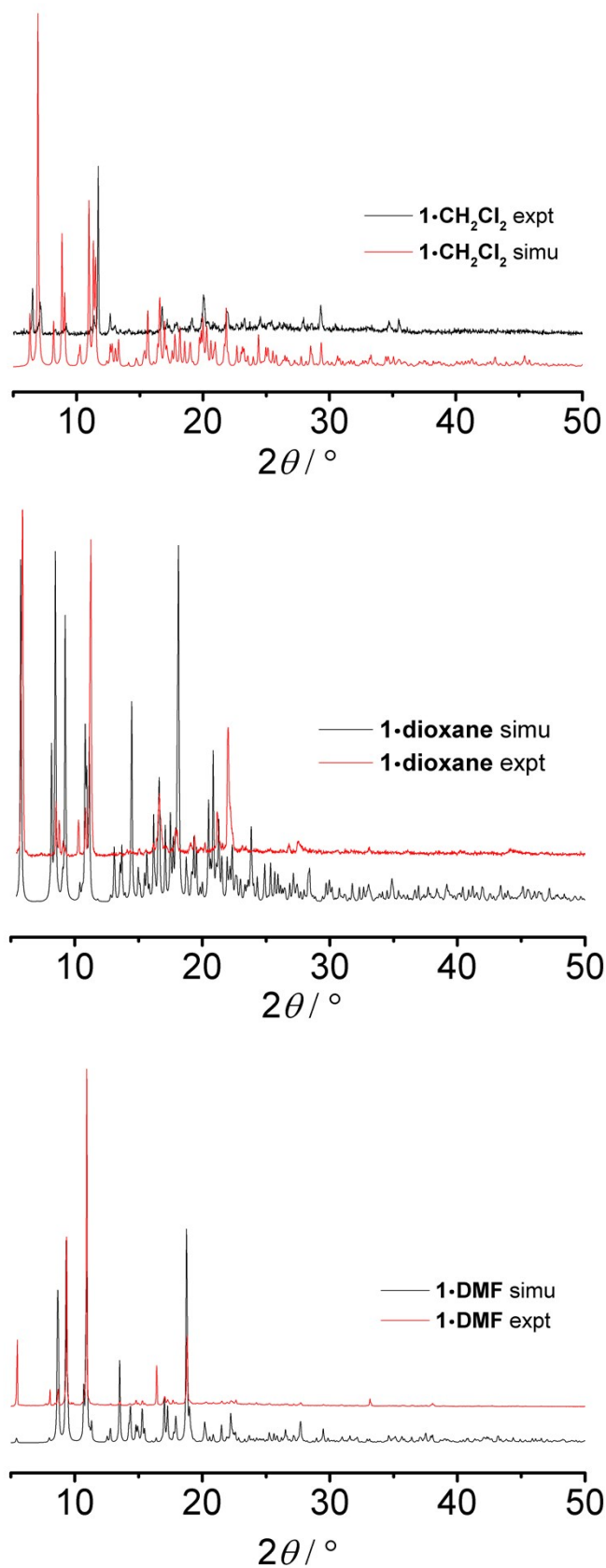


Figure S1. Room-temperature powder X-ray diffraction of $1\cdot\text{CH}_2\text{Cl}_2$, $1\cdot\text{dioxane}$, and $1\cdot\text{DMF}$.

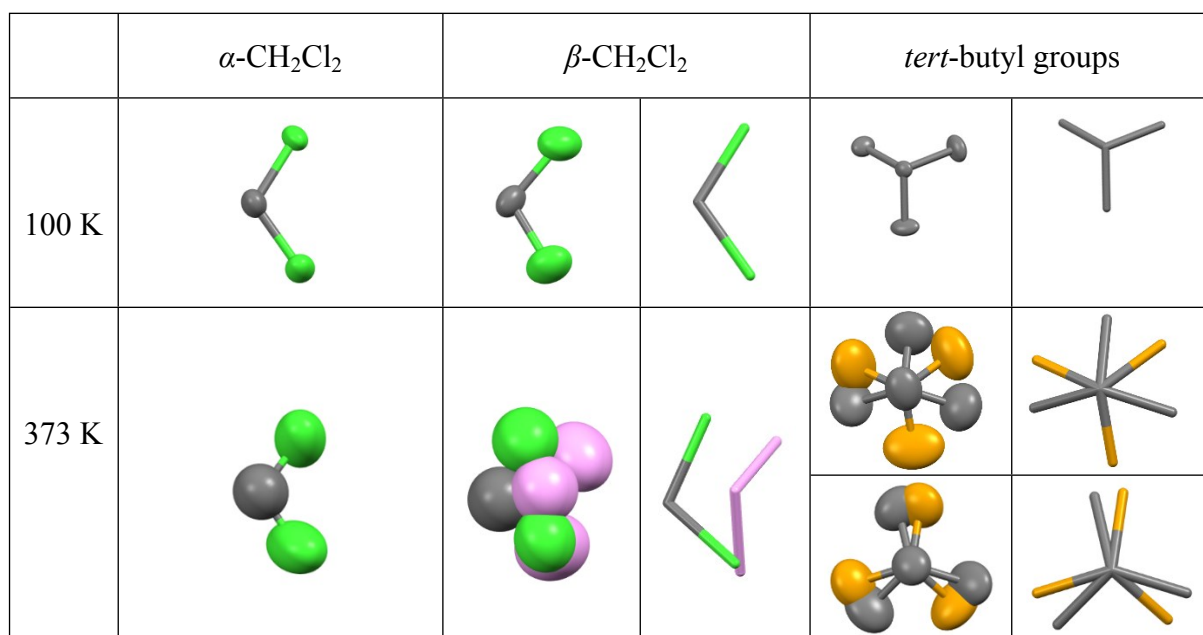


Figure S2. Two-site disorders of α -CH₂Cl₂ and β -CH₂Cl₂ molecules and one *tert*-butyl group of **1**·CH₂Cl₂.

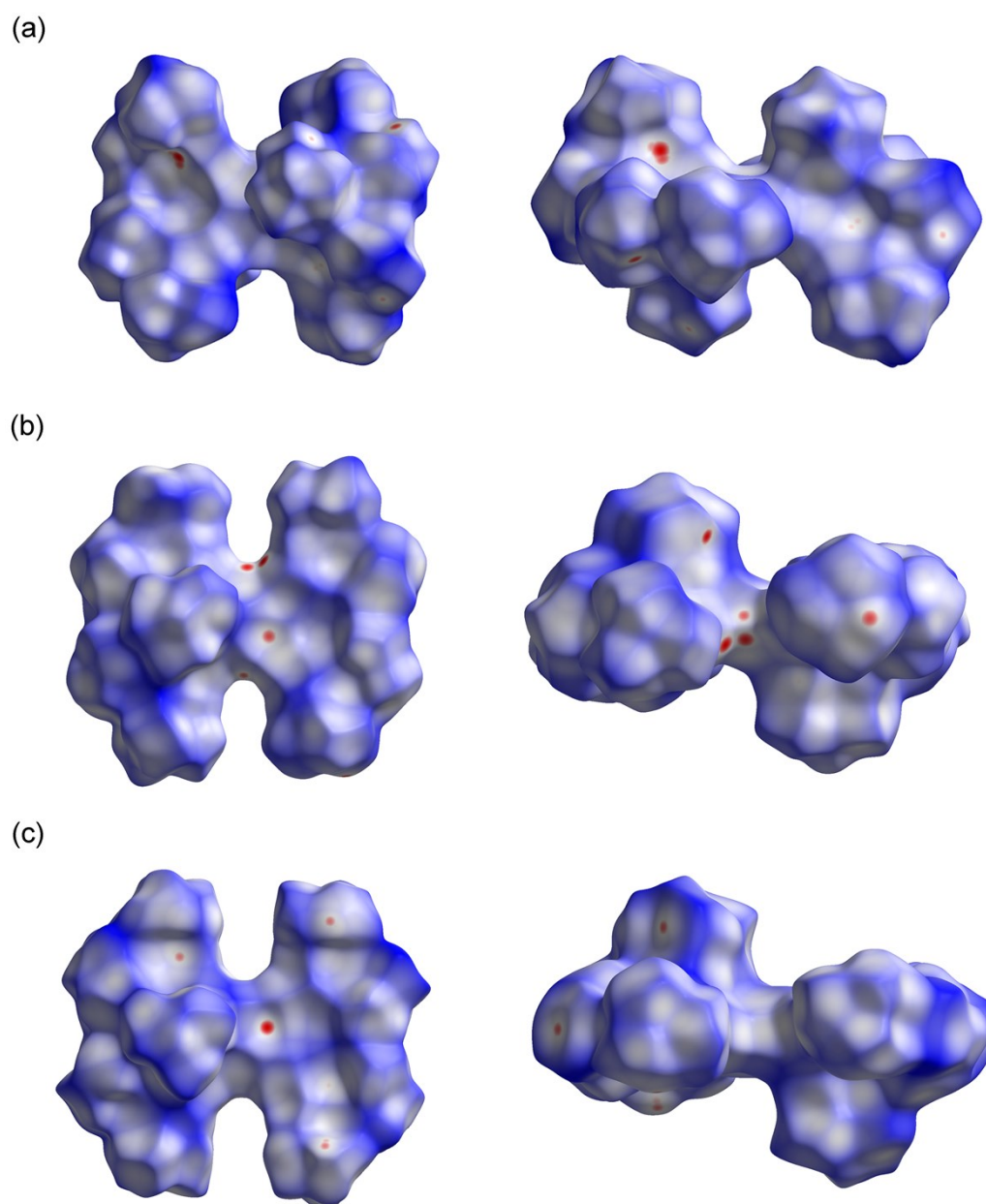


Figure S3. Atomic contacts to the Hirshfeld surface of the $[\text{Zn}_2(\text{saloph})]$ of crystals $1 \cdot \text{CH}_2\text{Cl}_2$, $1 \cdot \text{dioxane}$, and $1 \cdot \text{DMF}$.

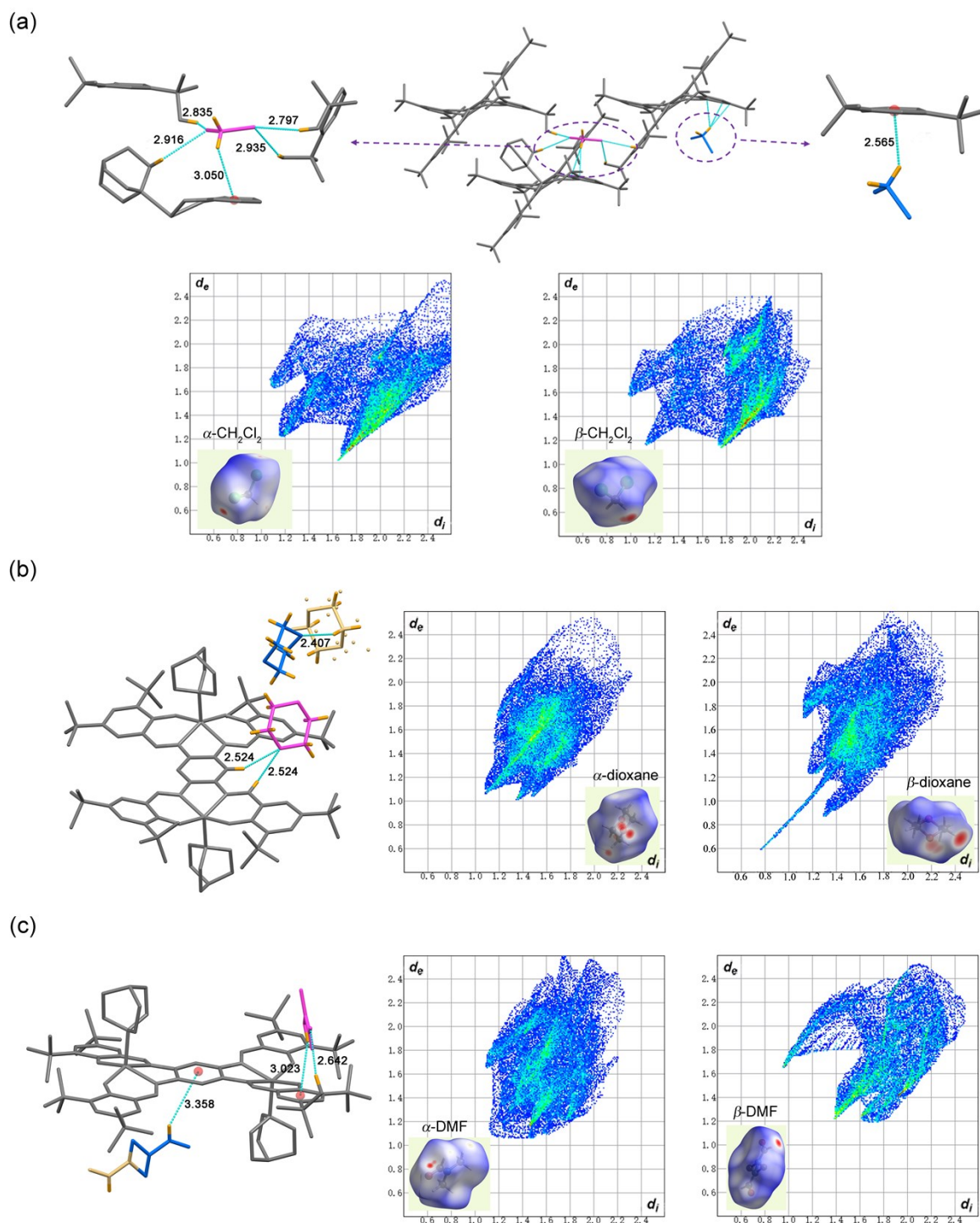


Figure S4. Intermolecular interactions between the guest and host and Hirshfeld surface analysis together with fingerprint plots of (a) $1 \cdot \text{CH}_2\text{Cl}_2$, (b) $1 \cdot \text{dioxane}$, and (c) $1 \cdot \text{DMF}$ at 100 K. H atoms involved in the interactions are shown in orange. The blue, white, and red regions of the surfaces correspond to negative, neutral, and positive (close contact) isoenergy, respectively.

To understand the high thermal stability of the CH_2Cl_2 solvate $\mathbf{1}\cdot\text{CH}_2\text{Cl}_2$, we firstly analyze the $\text{CH}\cdots\pi$ and $\text{CCl}\cdots\text{H}$ intermolecular interactions between the guest and host molecules 100 K by Hirshfield surface analysis (Figure S4a). Both the α - and β - CH_2Cl_2 molecules are encapsulated in the voids in isolated pairs. For the α - CH_2Cl_2 , the involved $\text{H}\cdots\text{C}_{\text{centroid}}$ (phenyl ring) distance in the $\text{CH}\cdots\pi$ is 3.050 Å while the $\text{Cl}\cdots\text{H}$ distances in the halogen bonds are between 2.797 and 2.935 Å. The β - CH_2Cl_2 only has $\text{CH}\cdots\pi$ bonds with the lengths between 2.565 Å. In $\mathbf{1}\cdot\text{dioxane}$, the α -dioxane only have weak $\text{CH}\cdots\text{O}$ interactions with the host molecules and β -dioxane 100 K (Figure S4b). The distances of the H to atoms O are 2.524, 2.524, and 2.407 Å. Furthermore, in $\mathbf{1}\cdot\text{DMF}$, The $\text{O}\cdots\text{H}$ distance in the $\text{CH}\cdots\text{O}$ hydrogen bonds is 2.642 Å. The α -DMF and β -DMF have weak $\text{CH}\cdots\pi$ bonds with the $\text{H}\cdots\text{C}_{\text{centroid}}$ distances of 3.358 and 3.023 Å (Figure S4c). Comparing to $\mathbf{1}\cdot\text{DMF}$, the guests of $\mathbf{1}\cdot\text{CH}_2\text{Cl}_2$ show more red regions, revealing more closer contacts, and fingerprint plots validate this result (Figure S4a, S4c). The maximal surface of red regions and the sharp fingerprint plot of β -dioxane in $\mathbf{1}\cdot\text{dioxane}$ indicate seemingly stronger intermolecular interactions. While it is an illusion caused by calculation results. Since the interplay is between the β -dioxane and γ -dioxane which are closely packing not the β -dioxane guest and the host-plate. These results reflect the different cavity environments of the confined three types of guest molecules. All them show weak interaction between the host molecule and the guest solvent molecules.

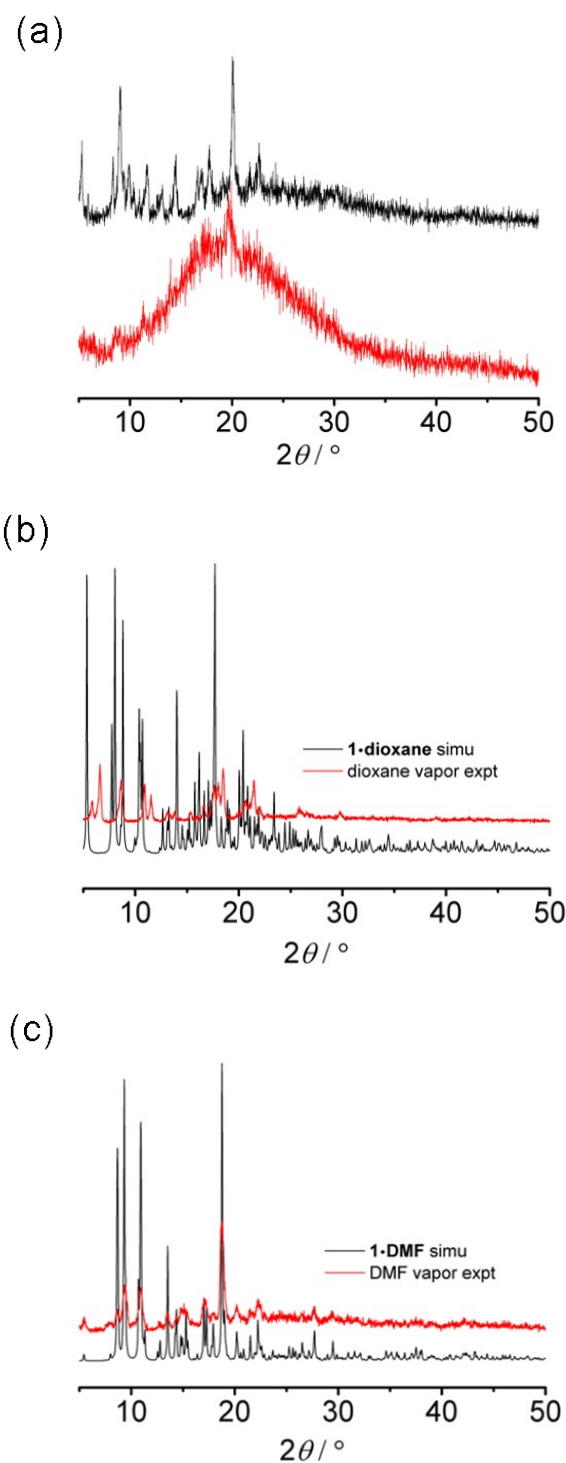


Figure S5 (a) The XRD pattern of the desolvated form from **1·DMF** measured with Kapton film protection (red curve) and in ambient (black curve). The re-adsorption experiment for dioxane (b) and DMF (c). The desolvate compound **1** was placed under the dioxane vapor (433 K) and DMF vapor (433 K) for 2h. After that, XRD measurement was employed to check the final component. Compound **1** can't turn back to **1·dioxane**, and it can turn back to **1·DMF**.

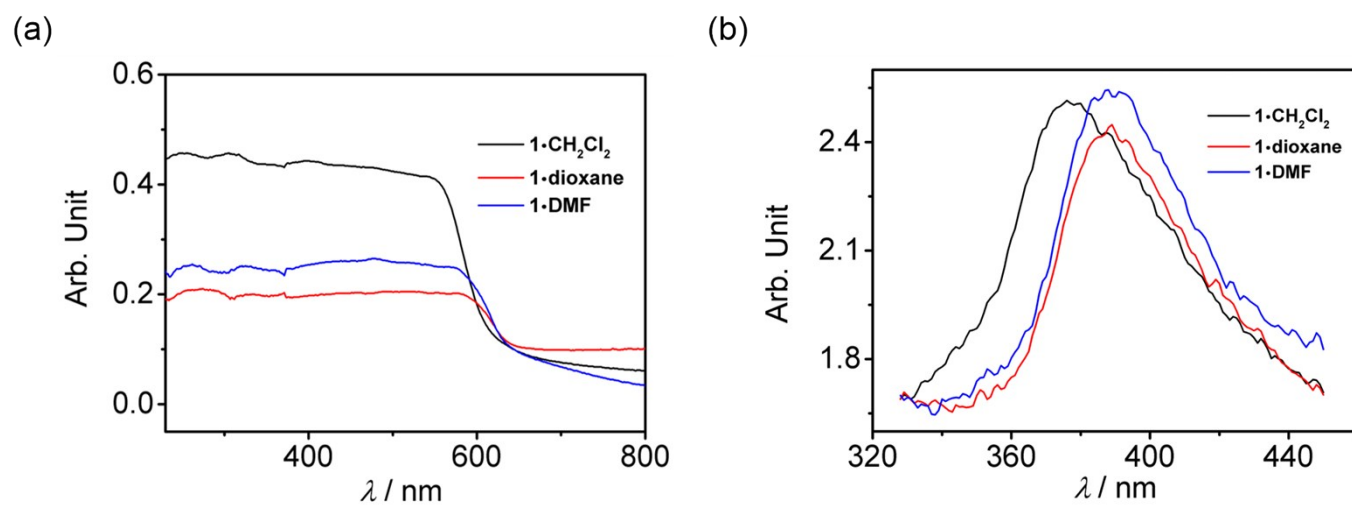


Figure S6 The UV-vis diffuse reflectance spectra (a) and the excitation spectra (b) of three compounds.

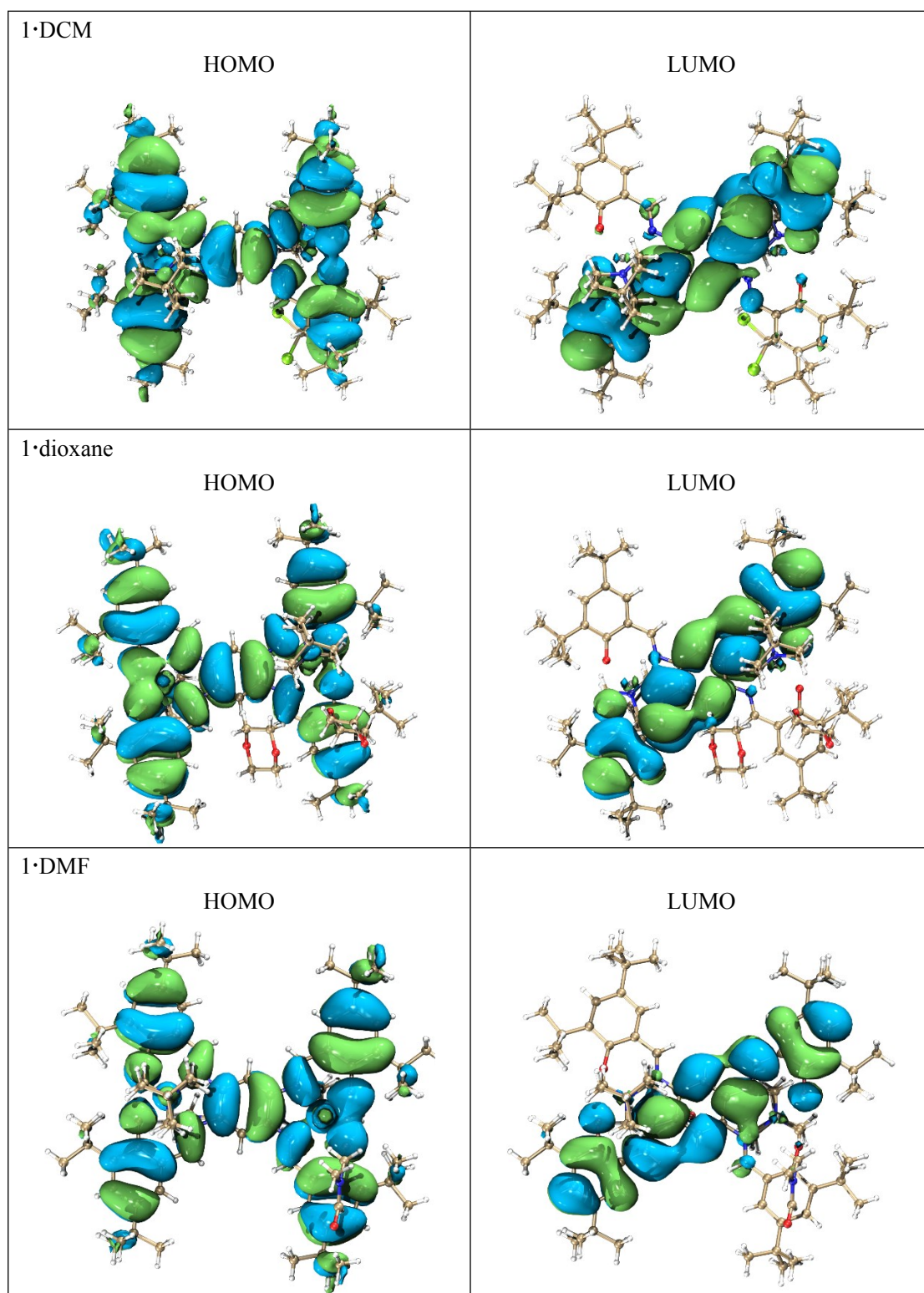


Figure S7 The calculated HOMO and HOMO for three compounds.

Table S1. Crystallographic data and structure refinement details for **1·CH₂Cl₂**, **1·dioxane**, and **1·DMF**.

1·CH₂Cl₂	100 K	153 K	253 K	293 K
formula	C ₈₄ H ₁₂₀ N ₆ O ₄ Zn ₂ Cl ₈	C ₈₄ H ₁₂₀ N ₆ O ₄ Zn ₂ Cl ₈	C ₈₄ H ₁₂₀ N ₆ O ₄ Zn ₂ Cl ₈	C ₈₄ H ₁₂₀ N ₆ O ₄ Zn ₂ Cl ₈
M_w	1692.24	1692.24	1692.24	1692.24
Crystal system	Monoclinic	Monoclinic	Monoclinic	Monoclinic
space group	$P2_1/n$	$P2_1/n$	$P2_1/n$	$P2_1/n$
diffraction source	Mo K α	Mo K α	Mo K α	Mo K α
wavelength [nm]	0.71073	0.71073	0.71073	0.71073
a [Å]	11.0806(2)	11.0967(2)	11.1134(2)	11.1207(3)
b [Å]	14.0971(3)	14.1310(3)	14.2035(3)	14.2524(3)
c [Å]	27.4716(6)	27.5930(6)	28.0547(7)	28.2337(7)
α [°]	90	90	90	90
β [°]	96.807(2)	97.044(2)	98.077(2)	98.503(2)
γ [°]	90	90	90	90
V [Å ³]	4260.93(15)	4294.13(15)	4384.48(17)	4425.76(19)
Z	2	2	2	2
ρ_{calcd} [g cm ⁻³]	1.319	1.309	1.282	1.270
μ [mm ⁻¹]	0.865	0.858	0.841	0.833
total reflns	45339	47513	43810	47105
obsd reflns ($I > 2\sigma(I)$)	12925	13072	13265	13332
R_{int}	0.0385	0.0361	0.1270	0.0406
$R_1^{\text{[a]}}$, $wR_2^{\text{[b]}}$ ($I > 2\sigma(I)$)	0.0806, 0.2378	0.0775, 0.2290	0.0830, 0.2268	0.0635, 0.1919
$R_1^{\text{[a]}}$, $wR_2^{\text{[b]}}$ (all data)	0.0954, 0.2496	0.0953, 0.2421	0.1100, 0.2477	0.0980, 0.2144
GOF (F^2)	1.045	1.036	1.046	1.048
$\Delta\rho^{\text{[c]}}$ [e Å ⁻³]	3.062 / -2.410	2.063 / -2.030	1.065 / -1.780	0.741 / -0.728

1·CH₂Cl₂	333 K	373 K
formula	C ₈₄ H ₁₂₀ N ₆ O ₄ Zn ₂ Cl ₈	C ₈₄ H ₁₂₀ N ₆ O ₄ Zn ₂ Cl ₈
M_w	1692.24	1692.24
Crystal system	Monoclinic	Monoclinic
space group	<i>P2₁/n</i>	<i>P2₁/n</i>
diffraction source	Mo K α	Mo K α
wavelength [nm]	0.71073	0.71073
a [Å]	11.1435(3)	11.1720(3)
b [Å]	14.3229(4)	14.4058(3)
c [Å]	28.3951(9)	28.4891(8)
α [°]	90	90
β [°]	98.853(3)	99.187(2)
γ [°]	90	90
V [Å ³]	4478.1(2)	4526.3(2)
Z	2	2
ρ_{calcd} [g cm ⁻³]	1.255	1.242
μ [mm ⁻¹]	0.823	0.814
total reflns	47289	43829
obsd reflns ($I > 2\sigma(I)$)	13457	13718
R_{int}	0.0438	0.0383
$R_1^{\text{[a]}}$, $wR_2^{\text{[b]}}$ ($I > 2\sigma(I)$)	0.0648, 0.1934	0.07752, 0.2266
$R_1^{\text{[a]}}$, $wR_2^{\text{[b]}}$ (all data)	0.1092, 0.2210	0.1224, 0.2553
GOF (F^2)	1.018	1.024
$\Delta\rho^{\text{[c]}}$ [e Å ⁻³]	0.561 / -0.726	0.658 / -0.667

	1·dioxane 100 K	1·DMF 100 K
formula	C ₁₀₄ H ₁₆₀ N ₆ O ₁₆ Zn ₂	C ₈₉ H ₁₃₃ N ₉ O ₇ Zn ₂
M_w	1881.16	1571.83
Crystal system	Monoclinic	Triclinic
space group	$P2_1/c$	$P\bar{1}$
diffraction source	Mo K α	Cu K α
wavelength [nm]	0.71073	1.54184
a [Å]	17.1238(6)	11.3185(5)
b [Å]	13.0894(4)	13.0309(5)
c [Å]	24.1334(9)	17.5656(6)
α [°]	90	110.595(4)
β [°]	105.365(4)	90.679(3)
γ [°]	90	115.103(4)
V [Å ³]	5215.9(3)	2156.09(17)
Z	2	1
ρ_{calcd} [g cm ⁻³]	1.198	1.206
μ [mm ⁻¹]	0.524	1.129
total reflns	49278	16185
obsd reflns ($I > 2\sigma(I)$)	15713	8763
R_{int}	0.0656	0.0250
$R_1^{[\text{a}]}$, $wR_2^{[\text{b}]}$ ($I > 2\sigma(I)$)	0.0987, 0.2915	0.0392, 0.1067
$R_1^{[\text{a}]}$, $wR_2^{[\text{b}]}$ (all data)	0.1601, 0.3384	0.0421, 0.1090
GOF (F^2)	1.048	1.074
$\Delta\rho^{[\text{c}]}$ [e Å ⁻³]	1.272 / -0.813	0.812 / -0.578

^[a] $R_1 = \Sigma ||F_o| - |F_c|| / |F_o|$. ^[b] $wR_2 = [\Sigma w(F_o^2 - F_c^2)^2] / \Sigma w(F_o^2)^2]^{1/2}$. ^[c] Maximum and minimum residual electron density.

Table S2. Selected bond lengths [\AA] and angles [$^\circ$] for **1**·**CH₂Cl₂** (100 K, 373 K), **1**·**dioxane** (100 K), and **1**·**DMF** (100 K).

1 · CH₂Cl₂ (100 K)			
N1–Zn1	2.111(3)	O1–Zn1–O2 ⁱ	100.92 (11)
N2–Zn1 ⁱ	2.100(3)	O1–Zn1–N2 ⁱ	146.74 (12)
N3–Zn1	2.103(3)	O2 ⁱ –Zn1–N2 ⁱ	84.98 (11)
O1–Zn1	1.956(3)	O1–Zn1–N3	102.44 (13)
O2–Zn1 ⁱ	2.005(3)	O2 ⁱ –Zn1–N3	98.45 (12)
Zn1–O2 ⁱ	2.005(3)	N2 ⁱ –Zn1–N3	109.07 (12)
Zn1–N2 ⁱ	2.100(3)	O1–Zn1–N1	88.63 (12)
		O2 ⁱ –Zn1–N1	157.71 (12)
		N3–Zn1–N1	76.34 (12)
		N1–Zn1–N2	99.08 (12)
1 · CH₂Cl₂ (373 K)			
N1–Zn1	2.127(3)	O1–Zn1–O2 ⁱ	101.64(10)
N2–Zn1 ⁱ	2.117(3)	O1–Zn1–N3	102.25(11)
N3–Zn1	2.112(3)	O2 ⁱ –Zn1–N3	98.85(11)
O1–Zn1	1.953(2)	O1–Zn1–N2 ⁱ	144.77(11)
O2–Zn1 ⁱ	1.992(2)	O2 ⁱ –Zn1–N2 ⁱ	84.55(9)
Zn1–O2 ⁱ	1.992(2)	N3–Zn1–N2 ⁱ	111.09(11)
Zn1–N2	2.117(3)	O1–Zn1–N1	87.40(10)
		O2 ⁱ –Zn1–N1	156.06(10)
		N3–Zn1–N1	100.81(11)
		N2 ⁱ –Zn1–N1	75.73(10)
1 · dioxane (100 K)			
N1–Zn1	2.111(4)	O1–Zn1–O2 ⁱ	92.95(16)
N2–Zn1 ⁱ	2.077(4)	O1–Zn1–N2 ⁱ	152.22(17)
N3–Zn1	2.106(5)	O2 ⁱ –Zn1–N2 ⁱ	88.99(16)
O1–Zn1	1.939(4)	O1–Zn1–N3	105.57(19)

O2-Zn1 ⁱ	1.963(4)	O2 ⁱ -Zn1-N3	101.6(2)
Zn1-O2 ⁱ	1.963(4)	N2 ⁱ -Zn1-N3	101.15(18)
Zn1-N2 ⁱ	2.077(4)	O1-Zn1-N1	87.80(15)
		O2 ⁱ -Zn1-N1	153.24(18)
		N2 ⁱ -Zn1-N1	78.44(16)
		N3-Zn1-N1	103.94(19)
1·DMF (100 K)			
N1-Zn1	2.1077(15)	O1-Zn1-O2	92.34(5)
N2-Zn1	2.0756(15)	O1-Zn1-N2	151.12(6)
N3-Zn1	2.1268(15)	O2-Zn1-N2	89.16(5)
O1-Zn1	1.9540(13)	O1-Zn1-N1	87.80(5)
O2-Zn1	1.9717(12)	O2-Zn1-N1	154.38(6)
		N2-Zn1-N1	78.81(6)
		O1-Zn1-N3	103.07(6)
		O2-Zn1-N3	103.73(6)
		N2-Zn1-N3	104.57(6)
		N1-Zn1-N3	101.18(6)

Table S3. The value of natural cavities and solvent molecules occupied volume of **1·CH₂Cl₂**, **1·dioxane**, and **1·DMF** calculated by Platon.

		Volume / Å ³	total unit cell volume / Å ³
1·CH₂Cl₂	Natural cavities	128.9	4260.9
	<i>α</i> -CH ₂ Cl ₂	254.8	
	<i>β</i> -CH ₂ Cl ₂	236.9	
	Total cavities	491.7	
1·dioxane	Natural cavities	79.1	5215.9
	Total cavities	2082.1	
1·DMF	Natural cavities	19.9	2156.1
	Total cavities	463.3	2156.1